

Crack Induced Stress and Generation of Twins and Dislocations in BCC Iron

Alena Spielmannová^{1, 2, a}, Anna Machová^{1, b}

¹Institute of Thermomechanics AS CR, v.v.i., Dolejškova 5, 18200 Prague 8, CR

²Dept. of Materials, FJFI-CTU, Trojanova 13, 12000 Prague 2, CR

^aspielmannova@it.cas.cz, ^bmachova@it.cas.cz

Keywords: stress calculations, anisotropic LEFM, crack orientation, twins, dislocations, bcc iron.

Abstract. We present new results of stress calculations in anisotropic continuum focused on generation of twins and dislocations at the crack front in bcc iron observed in 3D molecular dynamic (MD) simulations with edge cracks (001)[110] and ($\bar{1}10$)[110] (notation crack plane/crack front). The cracks are loaded in mode I. The stress calculations have been performed for plane strain and also plane stress conditions. This multiscale approach enable us to understand why the slip processes start at the free sample surface and why they are observed in MD both on the inclined and oblique slip planes to the crack front, similar to experimental observations on cracked iron crystals with low content of silicon.

Introduction

In this paper, crack induced stresses are calculated in the framework of linear elastic fracture mechanics (LEFM) utilizing the self-similar concept, including the K-factor and T-stress [1-3], and considering an anisotropic solid in order to make a comparison with the atomistic results as self-consistent as possible. No periodic boundary conditions have been used in our MD simulations [4] where the sample surfaces are free, except the loaded sample borders. At the free sample surfaces plane stress conditions prevail, while in the middle of the sample there are rather plane strain conditions, hence the stress analysis has been performed for both plane stress and plane strain.

The cracks considered in this paper (in atomistic simulations [4] and experiments [5, 6]) have non-zero initial crack opening, unlike the assumption in LEFM. However, the ratio of the crack length vs. half crack opening is $a/c/2 \gg 20$ and thus, according to Goodier's isotropic [7, 8] and also anisotropic solutions by Savin [3, 9] for elliptical cavities, they can be considered as the narrow cracks and treated by LEFM.

Stress analysis for inclined and oblique slip planes at the crack front

The crack tip stress field equations for mode I in anisotropic continuum with a basic coordinate system shown in Fig. 1 can be written [10] as

$$\begin{aligned}\sigma_{11} &= \frac{K_I}{\sqrt{2\pi r}} \operatorname{Re} \left\{ \frac{\mu_1 \mu_2}{\mu_1 - \mu_2} \left(\frac{\mu_2}{\sqrt{\cos \theta + \mu_2 \sin \theta}} - \frac{\mu_1}{\sqrt{\cos \theta + \mu_1 \sin \theta}} \right) \right\}, \\ \sigma_{22} &= \frac{K_I}{\sqrt{2\pi r}} \operatorname{Re} \left\{ \frac{1}{\mu_1 - \mu_2} \left(\frac{\mu_1}{\sqrt{\cos \theta + \mu_2 \sin \theta}} - \frac{\mu_2}{\sqrt{\cos \theta + \mu_1 \sin \theta}} \right) \right\}, \\ \sigma_{12} &= \frac{K_I}{\sqrt{2\pi r}} \operatorname{Re} \left\{ \frac{\mu_1 \mu_2}{\mu_1 - \mu_2} \left(\frac{1}{\sqrt{\cos \theta + \mu_1 \sin \theta}} - \frac{1}{\sqrt{\cos \theta + \mu_2 \sin \theta}} \right) \right\},\end{aligned}\tag{1}$$

where μ_1 and μ_2 are complex variables and they represent conjugate pair of roots from the compatibility equation

$$A_{11}\mu^4 - 2A_{16}\mu^3 + (2A_{12} + A_{66})\mu^2 - 2A_{26}\mu + A_{22} = 0 \quad (2)$$

The symmetric compliance constants A_{ij} describe [10] the strain-stress relations in anisotropic medium. In the case of cubic crystals $A_{16} = A_{26} = 0$.

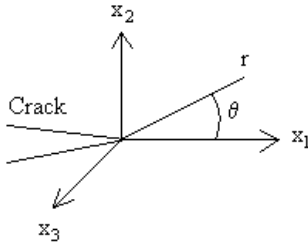


Fig. 1 Basic coordinate system

Under plane strain conditions A_{ij} can be found from the ‘unconstrained’ compliances s_{ij} for cubic crystals and from the condition $\epsilon_{33} = 0 = s_{31}\sigma_{11} + s_{32}\sigma_{22} + s_{33}\sigma_{33}$ determining also the third stress component σ_{33} . Under plane stress the constants A_{ij} are identical with s_{ij} . Since the constants A_{ij} are different for plane strain and plane stress, also the complex variables μ_1, μ_2 will differ.

Our stress analysis is based on comparison of the slip stress τ_b (acting on the slip plane in the direction of the Burgers vector b) with the critical stress needed either for twin generation τ_{twin} or dislocation emission τ_{dist} . The slip stress τ_b can be calculated from the crack tip stress field by LEFM after corresponding transformation of the coordinate system, while the critical stresses τ_{twin} and τ_{dist} are ‘materials’ parameters determined from the block like shear (BLS) simulations [11] with the interatomic potential used in our MD simulations [12, 13].

The T -stress acts parallel with the crack plane and it can modify the value of the critical slip stress τ_{twin} and τ_{dist} respectively according to scheme by Rice [1]: $\tau_c \rightarrow \tau_c + T \sin \theta \cos \theta$, if the slip system is inclined at angle θ as in Fig. 1. If not, then the angular function staying at T will be the same as for the stress component σ_{11} after the coordinate transformation. If T is negative, then it decreases the critical values τ_{twin} and τ_{dist} . The T -stress for our finite sample geometry is approximated according [2] by the relation

$$\frac{T}{\sigma_A} = \frac{-0.526 + 0.641\alpha + 0.2049\alpha^2 + 0.755\alpha^3 - 0.7974\alpha^4 + 0.1966\alpha^5}{(1-\alpha)^2} = -0.61399, \quad (3)$$

where $\alpha = l_0 / W = 0.3$ and l_0 and W are the initial crack length and sample width respectively, σ_A is the applied stress. In MD simulations, the mentioned slip processes are observed close to the critical (Griffith) level of the applied stress, hence in our stress analysis we calculate with the applied stress

$$\sigma_A = \sigma_{cr} = K_G / (F_I \sqrt{\pi l_0}). \quad (4)$$

Here $F_I = 1.27$ is a boundary correction factor by Harris [14], K_G is a critical stress intensity for cleavage crack initiation defined [10] by the relation $2\gamma = CK_G^2$, where $\gamma = \gamma_{001} = 1.812 \text{ Jm}^{-2}$ and $\gamma = \gamma_{110} = 1.585 \text{ Jm}^{-2}$ are the surface formation energies [12] for the cracks (001) and $(\bar{1}10)$ respectively and $C = \sqrt{A_{11}A_{22}/2} \sqrt{\sqrt{A_{22}/A_{11}} + (2A_{12} + A_{66})/2A_{11}}$, [10].

Twinning and dislocation emission in MD simulations [4] were observed both on the inclined and oblique slip planes. The inclined slip plane contains the crack front, while the oblique slip plane intersects the crack front. The angle θ in Fig. 1 and Eq. 1 can be determined [15] in both cases as the angle between the direction of potential crack extension and the intersection of the slip plane with the front plane of the sample. This will be explained more in detail in the next subsections devoted to the individual crack orientations.

The values τ_b are determined for three different distances r from the crack front. In the case of slip systems oriented in the easy twinning direction, the maximum τ_{twin} is reached [11] at the distance $r = b/10$, where $b = a_0\sqrt{3}/2 = 2.482462 \times 10^{-10} \text{ m}$ is Burgers vector in bcc iron. As to τ_{disl} , its maximum lies [11] at the distance $r = b/4$. Further, the values τ_b are calculated for $r = b/2$ and $r = b$.

Crack orientation (001)[110]

Here we associate the Cartesian axes (x_1, x_2, x_3) from Fig. 1 with the crystallographic directions $[\bar{1}10]$, $[001]$ and $[110]$. According to MD simulations [4], the following slip systems will be considered: the oblique slip system $\langle 111 \rangle \{011\}$ (Fig. 2a), the inclined slip system $\langle 111 \rangle \{112\}$ (Fig. 2b) and the oblique slip system $\langle 111 \rangle \{112\}$. Fig. 2 shows that both the oblique slip system $\{011\}$ and the inclined slip system $\{112\}$ create the angle $\theta = 35.26439^\circ$ since $\cos \theta = \sqrt{2/3}$.

For the oblique slip system $\langle 111 \rangle \{112\}$ in Fig. 3, the angle θ is zero. The blue arrows in Fig. 2 and Fig. 3 denote the Burgers vector in bcc iron.

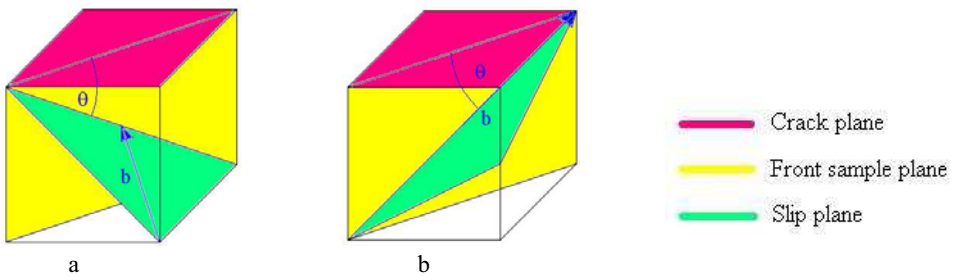


Fig. 2 a) Oblique slip system $\langle 111 \rangle \{011\}$, b) Inclined slip system $\langle 111 \rangle \{112\}$

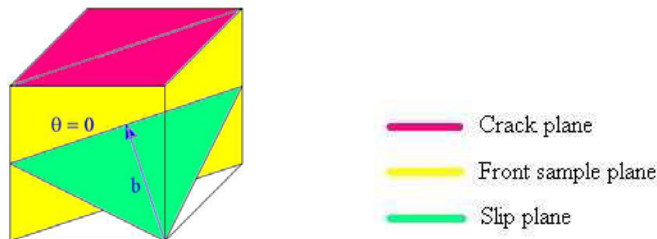


Fig. 3 Oblique slip system $\langle 111 \rangle \{112\}$

The basic matrix of the elastic constants C for crack orientation (001) is given in [12]. The matrix S of elastic compliances can be obtained by inversion of C and used for A_{ij} calculations according to procedure described e.g. in [10].

Plane strain (PD) conditions: The elastic compliances A_{ij} for the crack orientation (001)[110] are $A_{11} = 0.4470$, $A_{22} = 0.5698$, $A_{12} = -0.2664$ and $A_{66} = 0.8621$ in units of $10^{-11} \text{ m}^2/\text{N}$. Corresponding complex roots of Eq. 2 are $\mu_1 = 0.6167 + 0.8653i$ and $\mu_2 = -0.6167 + 0.8653i$. The stress components σ_{11} , σ_{22} , σ_{12} and σ_{33} in the original coordinate system $x_1 = [\bar{1}10]$, $x_2 = [001]$, $x_3 = [110]$ are determined by Eq. 1 and by the condition $\varepsilon_{33} = 0$ and are described by Eq. 5 and Eq. 6 below.

a) inclined slip plane {112} and oblique slip plane {011}

$$\sigma_{11} = 0.872 \frac{K_I}{\sqrt{2\pi r}}, \sigma_{22} = 1.207 \frac{K_I}{\sqrt{2\pi r}}, \sigma_{12} = 0.223 \frac{K_I}{\sqrt{2\pi r}}, \sigma_{33} = 0.715 \frac{K_I}{\sqrt{2\pi r}}. \quad (5)$$

b) oblique slip plane {112}

$$\sigma_{11} = 1.129 \frac{K_I}{\sqrt{2\pi r}}, \sigma_{22} = \frac{K_I}{\sqrt{2\pi r}}, \sigma_{12} = 0, \sigma_{33} = 0.577 \frac{K_I}{\sqrt{2\pi r}}. \quad (6)$$

Plane stress (PS) conditions: The elastic compliances for the crack orientation (001)[110] are $A_{11} = 0.4475$, $A_{22} = 0.7409$, $A_{12} = -0.2767$, $A_{66} = 0.8621$ in units of $10^{-11} \text{ m}^2/\text{N}$. Corresponding complex roots of Eq. 2 are $\mu_1 = 0.6863 + 0.9032i$ and $\mu_2 = -0.6863 + 0.9032i$. In the same way as above we determine the stress components from Eq. 1 and obtain for:

a) inclined slip plane {112} and oblique slip plane {011}

$$\sigma_{11} = 0.960 \frac{K_I}{\sqrt{2\pi r}}, \sigma_{22} = 1.209 \frac{K_I}{\sqrt{2\pi r}}, \sigma_{12} = 0.234 \frac{K_I}{\sqrt{2\pi r}}. \quad (7)$$

b) oblique slip plane {112}

$$\sigma_{11} = 1.287 \frac{K_I}{\sqrt{2\pi r}}, \sigma_{22} = \frac{K_I}{\sqrt{2\pi r}}, \sigma_{12} = 0. \quad (8)$$

Inclined slip systems <111>{112}: To calculate τ_b for the inclined slip system $[\bar{1}11]$ ($1\bar{1}2$) we introduce a new coordinate system $x'_1 = [\bar{1}11]$, $x'_2 = [1\bar{1}2]$, $x'_3 = [110]$. The slip stress in the new coordinate system is $\tau_b = \sigma'_{12} = a_{11}a_{21}\sigma_{11} + a_{12}a_{22}\sigma_{22} + (a_{11}a_{22} + a_{12}a_{21})\sigma_{12}$, where a_{ij} are the directional cosines of the transformation. It gives

$$\tau_b = \sqrt{2}(\sigma_{22} - \sigma_{11})/3 + \sigma_{12}/3. \quad (9)$$

Supposing that $K_I = K_G$, where

$$K_G^{PD} = 0.912 \text{ MPa}\times\text{m}^{1/2}, K_G^{PS} = 0.835 \text{ MPa}\times\text{m}^{1/2}, \quad (10)$$

Eq. 5 and Eq. 7 are utilized to evaluate the slip stress in the inclined slip systems <111>{112} under plane strain (τ_b^{PD}) and plane stress (τ_b^{PS}) conditions – see Table 1.

r	τ_b^{PD} [GPa]	τ_b^{PS} [GPa]
$b/10$	16.97	13.13
$b/2$	7.59	5.87
b	5.37	4.15

Table 1 Slip stress τ_b for the inclined planes $\{112\}$

The inclined slip systems $\langle 111 \rangle \{112\}$ are oriented in the easy twinning direction, where the barrier for twin generation with the potential used is $\tau_{twin} = 9.3$ GPa [11] but it can be decreased according to Rice correction $\tau_c \rightarrow \tau_c + T \sin \theta \cos \theta$. In this case $\theta = 35.26439^\circ$, the initial crack length in MD is $l_0 = 46 \times a_0 \sqrt{2}/2$ and the critical applied stress corresponding plane strain and plane stress is $\sigma_{cr}^{PD} = 4.196$ GPa and $\sigma_{cr}^{PS} = 3.842$ GPa respectively. In MD the inclined twins appear only under fast loading when plane strain conditions prevail [4]. Taking in Eq. 3 $\sigma_A = \sigma_{cr}^{PD} = 4.196$ GPa we obtain $T = -2.576$ GPa and the corrected value of the critical stress is $\tau_{twin} = 8.09$ GPa. From the comparison of the slip stress τ_b in Table 1 with the corrected value τ_{twin} we can see that the twinning at the crack (001)[110] is possible also according to LEFM, which is in agreement with MD results.

Oblique slip systems $\langle 111 \rangle \{112\}$: The new coordinate system is introduced according to Fig. 3, i.e. $x'_1 = [\bar{1}10]$, $x'_2 = [112]$, $x'_3 = [\bar{1}\bar{1}1]$. After the coordinate and stress transformation we obtain the slip stress $\tau_b = \sigma'_{23} = a_{2i}a_{3j}\sigma_{ij} = a_{22}a_{32}\sigma_{22} + a_{23}a_{33}\sigma_{33}$. Due to the component σ_{33} , different expressions are valid for plane strain and plane stress:

$$\tau_b^{PD} = \sqrt{2}(\sigma_{22} - \sigma_{33})/3, \quad \tau_b^{PS} = \sqrt{2}\sigma_{22}/3. \quad (11)$$

Utilizing Eq. 6, Eq. 8 and $K_I = K_G$ from Eq. 10, we obtain the slip stress for plane strain and plane stress conditions – see Table 2.

r	τ_b^{PD} [GPa]	τ_b^{PS} [GPa]
$b/10$	14.57	31.55
$b/2$	6.52	14.11
b	4.61	9.98

Table 2 Slip stress τ_b for the oblique planes $\{112\}$

The oblique slip systems $\langle 111 \rangle \{112\}$ in Fig. 3 are oriented in the easy twinning direction. Since Eq. 11 does not contain the stress component σ_{11} there is no T -stress correction needed and the stress barrier for twin generation is $\tau_{twin} = 9.3$ GPa from [11]. When comparing the value of τ_{twin} with the values of τ_b in Table 2 we can see that twinning on the oblique planes $\{112\}$ at the crack (001) is possible according to LEFM for both plane strain and plane stress conditions. Oblique twinning is more favorable for plane stress conditions, which is in qualitative agreement with MD, where this condition prevails under slow loading.

Oblique slip systems $\langle 111 \rangle \{011\}$: According to Fig. 2a, a new coordinate system is chosen as $x'_1 = [011]$, $x'_2 = [21\bar{1}]$, $x'_3 = [\bar{1}\bar{1}1]$. After the transformation of the stress tensor, we obtain the slip stress $\tau_b = \sigma'_{13} = a_{1i}a_{3j}\sigma_{ij} = a_{11}a_{32}\sigma_{12} + a_{12}a_{32}\sigma_{22} + a_{13}a_{33}\sigma_{33}$. It leads to the following expressions

$$\tau_b^{PD} = \sqrt{3}\sigma_{12}/6 + \sqrt{6}\sigma_{22}/6 - \sqrt{6}\sigma_{33}/6, \tau_b^{PS} = \sqrt{3}\sigma_{12}/6 + \sqrt{6}\sigma_{22}/6. \quad (12)$$

Using Eq. 5 and Eq. 7 and $K_I = K_G$ from Eq. 10, we obtain the slip stress for plane strain and plane stress conditions, see Table 3:

r	τ_b^{PD} [GPa]	τ_b^{PS} [GPa]
$b/4$	12.26	23.75
$b/2$	8.67	16.79
b	6.13	11.88

Table 3 Slip stress τ_b for oblique planes $\{011\}$

The stress barrier for dislocation emission in the slip systems $\langle 111 \rangle \{011\}$ is relatively low [15], $\tau_{disl} = 14.5$ GPa. A comparison of the slip stress τ_b from Table 3 with τ_{disl} shows that dislocation emission on the oblique slip planes $\{011\}$ at the crack (001) is possible according to LEFM, namely under plane stress conditions that prevail in MD under slow loading [4]. Eq. 12 does not contain the stress component σ_{11} , hence the T-stress cannot influence the slip processes on the oblique planes $\{011\}$, similar to the oblique planes $\{112\}$.

Crack orientation ($\bar{1}10$)[110]

In this case only dislocation emission on the inclined slip systems $\langle 111 \rangle \{112\}$ oriented in the hard anti-twinning direction was observed in MD simulations [4]. That is the reason why our stress analysis is focused only on the inclined slip system $\langle 111 \rangle \{112\}$. Following relations are valid for the inclination angle in Fig. 4: $tg\theta = \sqrt{2}$, $\theta = 54.73561^\circ$.

Plane strain (PD) conditions: The constrained elastic compliances are $A_{11} = 0.5698$, $A_{22} = 0.4470$, $A_{12} = -0.2664$ and $A_{66} = 0.8621$ in units of 10^{-11} m²/N. The corresponding complex roots of Eq. 2 are $\mu_1 = 0.5462 + 0.7664i$ and $\mu_2 = -0.5462 + 0.7664i$. Note that in this case the fore mentioned values of A_{ij} and μ_{ij} are the same as presented in [3].

The original coordinate system from Fig. 1 has been chosen as $x_1 = [001]$, $x_2 = [\bar{1}10]$, $x_3 = [110]$. The corresponding stress components from Eq. 1 are

$$\sigma_{11} = 0.483 \frac{K_I}{\sqrt{2\pi r}}, \sigma_{22} = 1.304 \frac{K_I}{\sqrt{2\pi r}}, \sigma_{12} = 0.075 \frac{K_I}{\sqrt{2\pi r}}, \sigma_{33} = 0.250 \frac{K_I}{\sqrt{2\pi r}}. \quad (13)$$

Plane stress (PS) conditions: The unconstrained elastic compliances are $A_{11} = 0.7409$, $A_{22} = 0.4475$, $A_{12} = -0.2767$ and $A_{66} = 0.8621$ in units of 10^{-11} m²/N. The complex roots from Eq. 2 are $\mu_1 = 0.5333 + 0.7020i$ and $\mu_2 = -0.5333 + 0.7020i$. From Eq. 1 we obtain corresponding stresses

$$\sigma_{11} = 0.457 \frac{K_I}{\sqrt{2\pi r}}, \sigma_{22} = 1.333 \frac{K_I}{\sqrt{2\pi r}}, \sigma_{12} = 0.094 \frac{K_I}{\sqrt{2\pi r}}. \quad (14)$$

Inclined slip systems $\langle 111 \rangle \{112\}$: The new coordinate system is introduced in the following way $x'_1 = [1\bar{1}1]$, $x'_2 = [\bar{1}12]$, $x'_3 = [110]$. In the new coordinate system the slip stress is expressed as

$\tau_b = \sigma'_{12} = a_{11}a_{21}\sigma_{11} + a_{12}a_{22}\sigma_{22} + (a_{11}a_{22} + a_{12}a_{21})\sigma_{12}$ where a_{ij} are the directional cosines of the transformation. It leads to the relation

$$\tau_b = \sqrt{2}(\sigma_{22} - \sigma_{11})/3 - \sigma_{12}/3. \tag{15}$$

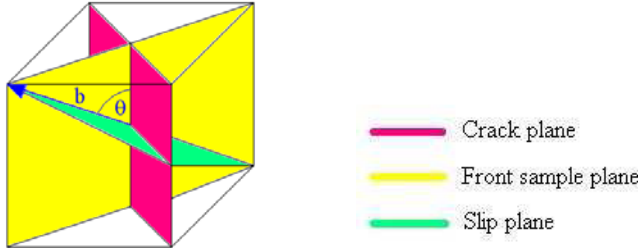


Fig. 4 Inclined slip system $\langle 111 \rangle \{112\}$

The critical values of the stress intensity for the crack orientation $(\bar{1}10)[110]$ under plane stress and strain conditions are

$$K_G^{PD} = 0.906 \text{ MPa}\times\text{m}^{1/2}, K_G^{PS} = 0.886 \text{ MPa}\times\text{m}^{1/2}. \tag{16}$$

Supposing that $K_I = K_G$ and using Eq. 14 and Eq. 15 we obtain the values of the slip stress τ_b in the inclined slip system $\langle 111 \rangle \{112\}$ at the crack $(\bar{1}10)[110]$ under plane strain and plane stress conditions given in Table 4.

r	τ_b^{PD} [GPa]	τ_b^{PS} [GPa]
$b/4$	16.61	17.12
$b/2$	11.75	12.10
b	8.31	8.56

Table 4 Slip stress τ_b for inclined planes $\{112\}$

Since the inclined slip systems $\langle 111 \rangle \{112\}$ at the crack $(\bar{1}10)$ are oriented in the hard anti-twinning direction, where the stress barrier for twin formation is very high ($\tau_{twin} = 27.9 \text{ GPa}$, [3]), it is more favorable for the crack to emit dislocations because of the lower stress barrier $\tau_{disl} = 16.3 \text{ GPa}$, [11]. Eq. 15 contains the stress component σ_{11} and so we may use the correction by Rice $\tau_{disl} = 16.3 \text{ GPa} + T \sin \theta \cos \theta$. The initial length of the crack $(\bar{1}10)$ is $l_0 = 66 \times a_0 / 2$ and the critical values of the applied stress under plane strain and plane stress conditions are $\sigma_{cr}^{PD} = 4.138 \text{ GPa}$ and $\sigma_{cr}^{PS} = 4.047 \text{ GPa}$ respectively. It decreases the stress barrier for dislocation generation to about $\tau_{disl} = 15.1 \text{ GPa}$. When comparing τ_{disl} with the slip stress τ_b in Table 4 we see that dislocation generation at the crack front of the crack $(\bar{1}10)$ is possible according to LEFM under plane strain and plane stress conditions as well. It explains why dislocation emission in MD was observed [4] both under fast (plane strain prevails) and also slow loading (plane stress prevail).

Note that real values of the slip stress presented in Tables 1 – 4 can be higher due to the nominal shear stress on $\{112\}$ or $\{110\}$ slip planes with large Schmid factor 0.47 and 0.41 respectively.

Summary

Our results show that higher stress level at the crack (001) in bcc iron is on the oblique slip planes in comparison with the inclined planes. It is in a qualitative agreement with the theoretical study [16] where the stresses were calculated by the finite element method. Larger slip stress prevails under plane stress conditions both at the crack (001) and $(\bar{1}10)$. It explains why the slip processes in MD start at the free sample surfaces. As to the crack $(\bar{1}10)$, dislocation emission according to LEFM is possible on the inclined slip planes $\{112\}$, in agreement with MD simulations.

The analysis is relevant for temperature of 0 K. At increased temperatures, a decline of the stress barrier τ_{disl} is expected due to the thermal activation (by about 20% in bcc iron at 300 K, [17]). The stress barrier for dislocation emission decreases also due to a fact that curved dislocations are emitted in 3D simulations [4] and also experiments since they have lower strain energy around. Both τ_{disl} [3] and τ_{twin} [18] come down also when normal relaxation occurs in the slip systems.

The results are in a qualitative agreement with our MD simulations [4] and experiments [5-6].

Acknowledgements: The work was supported by the Institute Research Plan AV0Z20760514 and by the grant KJB200760802.

References

- [1] J.R. Rice: *J. Mech. Phys. Solids* Vol. 22 (1974), p. 17
- [2] T. Fett: *A Compendium of T-stress solution* (Forschungszentrum Karlsruhe GmbH, Karlsruhe 1998, p. 34)
- [3] G.E. Beltz and A. Machová: *Modelling Simul. Mater. Sci. Eng.* Vol. 15 (2007), p. 65
- [4] A. Spielmannová, A. Machová and P. Hora: *Mater. Sci. Forum* Vol. 567-568 (2007), p. 61
- [5] J. Prah, A. Machová, M. Landa, P. Haušild, M. Karlík, A. Spielmannová, M. Clavel and P. Haghi-Ashtiani: *Mater. Sci. Eng. A* Vol. 462 (2007), p. 178
- [6] A. Spielmannová, M. Landa, A. Machová, P. Haušild, and P. Lejček: *Materials Characterization* Vol. 58 (2007), p. 892
- [7] J.N. Goodier, in: *Fracture* Vol. 2, edited by H. Liebowitz, Academic Press, New York (1968)
- [8] G.J. Dienes and A. Paskin: *J. Phys. Chem. Solids* Vol.48 (1987), p. 1015
- [9] G.N. Savin, in: *Stress Concentration Around Holes*, edited by G.N. Savin, Chapter 3, Pergamon Press, New York (1961)
- [10] H. Tada, B. Paris and G. Irwin: *The Stress Analysis Handbook* (Hellertown Del Research Corporation, Hellertown PA, 1973, D1-3)
- [11] A. Machová, G.E. Beltz and M. Chang: *Modell. Simul. Mater. Sci. Eng.* Vol. 7 (1999), p. 949
- [12] A. Machová and G.J. Ackland: *Modelling Simul. Mater. Sci. Eng.* Vol. 6 (1998), p. 521
- [13] G.J. Ackland, D.J. Bacon, A.F. Calder and T. Harry: *Phil. Mag. A* Vol. 75 (1997), p.713
- [14] D.O. Harris: *J. Bas. Engng. Trans. ASME, Series D*, Vol. B9 (1967), p.49
- [15] V. Pelikán, P. Hora, A. Machová and A. Spielmannová: *Czech.J.Phys.*Vol. 55 (2005), p. 1245
- [16] G. Xu and A.S. Argon: *Phil. Mag. A* Vol. 75 (1997), p. 341
- [17] J.R. Rice and G.E. Beltz: *J. Mech. Phys. Solids* Vol. 42 (1994), p. 333
- [18] V. Vitek: *Scripta Metallurgica: Vol. 4* (1970), p. 725